Formation of Klein Edge Doublets from Graphene Monolayers

Judy S. Kim,*,† Jamie H. Warner,† Alex W. Robertson,† and Angus I. Kirkland†,‡

†Department of Materials, University of Oxford, Parks Road, Oxford, OX13PH, U.K. and ‡Research Complex at Harwell (RCaH), Rutherford Appleton Laboratory Harwell, Didcot, Oxon, OX11 0FA, U.K.

ABSTRACT With increasing possibilities for applications of graphene, it is essential to fully characterize the rich topological variations in graphene edge structures. Using aberration-corrected transmission electron microscopy, dangling carbon doublets at the edge of monolayer graphene crystals have been observed. Unlike the single-atom Klein edge often found at zigzag edges, these carbon dimers were observed in various edge structure environments, but most frequently on the more stable armchair edges. Observation of this Klein edge doublet over time reveals that its existence enhances the stability of armchair edges and is a route to atom abstraction on zigzag edges.

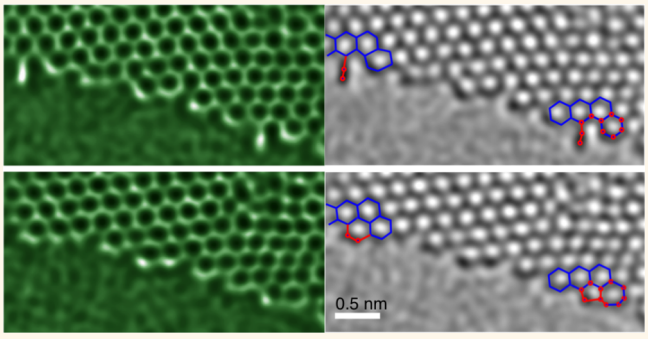

KEYWORDS: graphene · Klein edge doublet · radiation damage · transmission electron microscopy · monolayer · carbon dimer

Monolayer graphene has been studied extensively in recent years for a range of potential nanoscale applications that take advantage of its extraordinary mechanical and electronic transport properties.[1] Graphene edges have novel electronic properties compared to the bulk lattice, including localization lengths and elastic mean-free paths arising from varied local atomic topology at the edge,[2−5] and as a result have a significant effect on the overall behavior of edge-dominant graphene structures, such as nanoribbons.[6−27] Understanding these edge defects and the topology of monolayer graphene potentially enables the engineering of properties aimed at optimized performance. A number of prior studies have explored the rich variation in edge structures,[28−31] and changes in edge architecture have been shown to lead to variations in the local density of states[2,3,32,33] and work function for field electron emission.[34] In this paper we report a new edge structure that has not previously been observed experimentally. Our observation of the Klein edge doublet at the graphene edge is of interest due to the unique properties that arise from variations in differing edge terminations. The doublet is expected to perturb the local electronic density of states of the edge, resulting in analogous changes to the electronic and magnetic properties to those found in graphene nanoribbon edge terminations.[35] This new edge type is therefore an alternative option for the future nanoengineering of graphene devices.

Monolayer graphene was produced by atmospheric chemical vapor deposition (CVD) over a heated Cu substrate and subsequently removed using a $FeCl_3$ etchant and transferred to a perforated Si_3N_4 support grid using a poly(methyl methacrylate) (PMMA) scaffold.[36,37] Experimental aberration-corrected transmission electron microscopy (AC-TEM) images were recorded at room temperature using a JEOL 2200MCO[38−40] at 80 kV acceleration voltage, beneath the sputtering knock-on damage threshold for sp^2-bonded carbon.[41,42] Experimental AC-TEM imaging conditions were collected using optimized negative spherical aberration, C_3, imaging conditions[43] (see also Methods). Edges were created for the study by high current density electron beam irradiation of the target area.[37]

The Klein edge (KL) structure on graphene is often described as a single carbon or single hydrogen atom dangling from a zigzag-type edge. Klein established that this edge structure produces an unpaired electron

* Address correspondence to judy.kim@materials.ox.ac.uk.

Received for review May 6, 2015 and accepted August 18, 2015.

Published online August 18, 2015
10.1021/acsnano.5b02730

density of 2/3 e^- per cell.[44] Such single-carbon KLs have been previously observed.[2,3,28,30,45] We have also observed these structures numerous times in our specimens, but they are not the focus of this study. This work concentrates on the displacement of dangling carbon doublets at the graphene edge using time sequences of AC-TEM images. This type of extended Klein edge, measuring 0.23 ± 0.02 nm in length, consists of two C atoms attached in series to the graphene edges. Subsequently we refer to these structures as Klein edge doublets (KLD).

RESULTS AND DISCUSSION

The bond breakage and re-formation process of the KLD is first observed in two different armchair edge environments (Figure 1). One KLD is generated by the opening of a six-membered ring (Figure 1a,b, doublet is annotated *g* on the left), and the other forms from a reconstructed 5−7 ring (Figure 1a,b, doublet is annotated *h* on the right)). Both KLDs remain for two frames collected 6 s apart, where they open and shift position within the vacuum before rebonding to the armchair edge (Figure 1d). The stability of the C−C doublets is sufficient to withstand 80 kV electron beam irradiation at 2.5 × 10^6 e^-·s/nm^2 during the collection of two separate 2 s (acquisition time) images. Including the operator adjustment time between acquired frames, the KLDs remain for *ca.* 8 s under electron irradiation, exposing the specimen to ∼2.5 × 10^7 e^-/nm^2. Further observation under electron irradiation eventually causes the C edge atoms to sputter away (see Supporting Information Figure S2). Previous DFT/DFTB studies have suggested that the formation of these KLDs requires a displacement energy of 12.9 eV, 0.9 eV greater than that for a zigzag edge atom.[46] Our observations of both KLDs and the concurrent erosion of zigzag edge atoms lead us to infer that the experimental electron irradiation was sufficient to cause this displacement equivalent to 12.9 eV.

No carbon atoms are lost or gained in the local region around the KLD for an intrinsic disturbance of the crystal due to electron beam irradiation without the influence of foreign atoms on the local bonding structure. In addition, KLD formation and restitching into the graphene crystal lattice were dynamically observed in an edge-healing process (Figure 1). Observation of the dynamics of this healing process in the 0.5 × 10^{-5} Pa vacuum environment of the TEM suggests that it is unlikely an H atom terminates the KLD at any point. A previous study of a monolayer

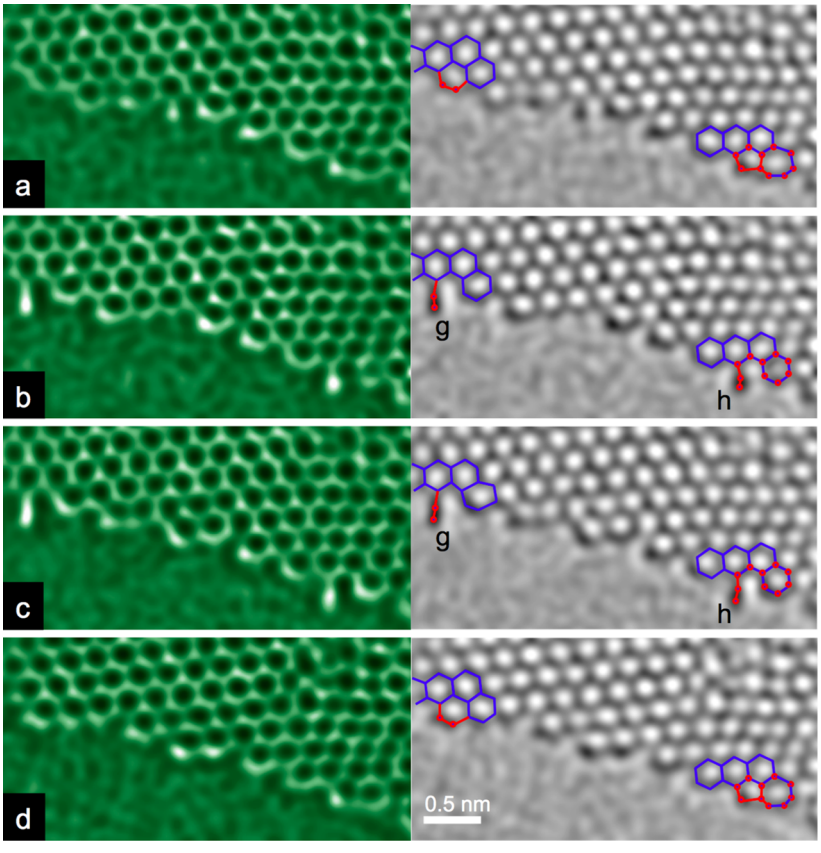

Figure 1. (a−d) Time series of AC-TEM images of a monolayer graphene sheet collected at 0, 6, 12, and 18 s, showing two Klein edge doublets forming from armchair terminated edges. The Klein doublets labeled *g* and *h* remain for two frames acquired for 2 s each, collected 6 s apart. (a)−(d) also show gray-scale images with a schematic overlay to highlight the local structure in the vicinity of the Klein doublets, where the blue lines represent the static portion of the structure and red lines highlight the dynamically changing bonds.

TABLE 1. Numerical Details of the Klein Edge Doublets (KLD) Shown in Figures 1−3

KLD name	shown in Figure	KLD length in TEM projection[a] (3 atoms) (nm)	KLD angle in TEM projection[a] (deg)	attached to edge type[b]	forms from ring type	attached to ring type
g	1b	0.221 ± 0.01	181.8 ± 7.0	AC	6	6
	1c	0.249 ± 0.01	195.5 ± 3.4			
h	1b	0.238 ± 0.02	191.2 ± 4.8	AC	5	6
	1c	0.213 ± 0.02	205.6 ± 6.8			
j	2	0.234 ± 0.01	172.1 ± 5.3	AC	6	5
k mixed composition	2	0.259 ± 0.01	150.1 ± 5.3	AC	6	6
m	3	0.238 ± 0.01	206.3 ± 5.0	ZZ	6	6
n	3	0.212 ± 0.01	168.1 ± 7.3	ZZ	6	6

[a] Lengths and angles of the KLDs are measured from AC-TEM images, which are 2D projections; therefore it is not possible to exclude any *z*-axis contribution to the apparent length. [b] AC and ZZ represent armchair and zigzag types, respectively.

graphene edge has shown that nonfunctionalized edges can exist in such an environment,[26] and in this case of dynamically observed KLDs, H functionalization could occur only in an elaborate series of events involving KLD formation, H bonding to the KLD tether, H−C bond breaking, and finally KLD reattaching to the bulk flake.

The existence of nonfunctionalized KLDs indicates the significance of controllable formation of a dangling σ bond on the edge of the graphene flake. This could enable the engineering of KLDs as dopant site receptors or nanodevice interconnects for practical application. Although KLD formation represents a transient state for the graphene edge morphology, it is not wholly unreasonable to give some weight to this proposal given the prolonged time scales over which the KLDs exist. This is a substantial time compared to that for the breakage of the C−C bond in a KLD (*ca.* 1.1 ps) in a graphene nanoribbon[47] in a high-temperature environment.

Considering the bonding within KLDs, an alternative model of a double- or triple-bond configuration along the dimer is unlikely, as the data show that the movement of the KLD does not maintain a 180° geometry (Table 1). Moreover, the presence of a dangling σ bond is consistent with the simulated restitching[46] of graphene edges that is known to occur at armchair edges.

Detailed examination of the images in this work reveals that there is a localized contrast change around atoms near the flake edge. This is evident in the bonded armchair edges, single KLs, and the KLDs. This may arise from a combination of the subtleties of image smoothing on low signal-to-noise ratio images of 3.74 (see Methods and Supporting Information Figure S2) and the more mobile edge atoms being located away from the *Z* plane of the main graphene crystal and the focus of the objective lens, giving rise to localized Fresnel fringe contrast at the edges. Similarly local intensity variations across the flake at the 2−3 nm scale may be due to undulations of the flake in the plane of the image.

Re-formation of armchair edges from KLDs has also been observed in a time-series experiment, revealing different behavior from that described above due to the contribution of extra atoms to the region of interest (Figure 2). The KLD (labeled *j* in Figure 2b) is 1.6 times the single C−C bond length in projection and is attached to a five-membered ring. However, we note that the measured bond length may represent only a component of the true bond length due to the potentially out-of-plane nature of the KLD. Our data show that one atom is added to the KLD formation site. This additional atom may originate from the adjacent edge containing the single KL visible in the first frame of the series. Single KL features on a zigzag edge have been previously observed to sputter from the main crystal,[30] and that appears to be a less stable configuration compared to KLD observed at armchair edges. The KLD (labeled *j* in Figure 2b) restructures into the main graphene flake after 8 s of electron beam irradiation, and it is apparent that one atom has joined the region of interest at the edge. This indicates that the KLD is an active site for bonding of free carbon atoms. Consequently, given that the displacement or formation energy of KLDs is a value discrete from that for displacement of a zigzag- or armchair-type edge atom, KLD formation can be used to form active bonding sites at the edge of monolayer graphene.

The image sequence shown in Figure 2 shows displacement of another KLD (labeled *k*) that is 0.26 ± 0.01 nm in length, with a strong intensity variation made evident in the profile of Figure 2d. We believe this to be the result of a heterogeneous composition (one C atom and one non-carbon adatom) KLD. The presence of heavier adatoms in this specimen has been previously confirmed in another study.[48] In particular, Fe can originate from the $FeCl_3$ etchant solution used during the fabrication process, and Si contamination can arise from the Si_3N_4 TEM grid and the CVD furnace environment generated within a quartz tube. Using multislice image simulations at an instrument defocus spread of 4 nm, the contrast ratio of adatom image intensity with a carbon atom was found to be Fe = 1.83, Si = 1.47, and Na = 1.25.[48] In this work, the intensity ratio of the adatom to average C intensity as collected from a box profile in Figure 2d is 1.45 ± 0.06 and is in good agreement with multislice simulations[48] of a Si to C atom.

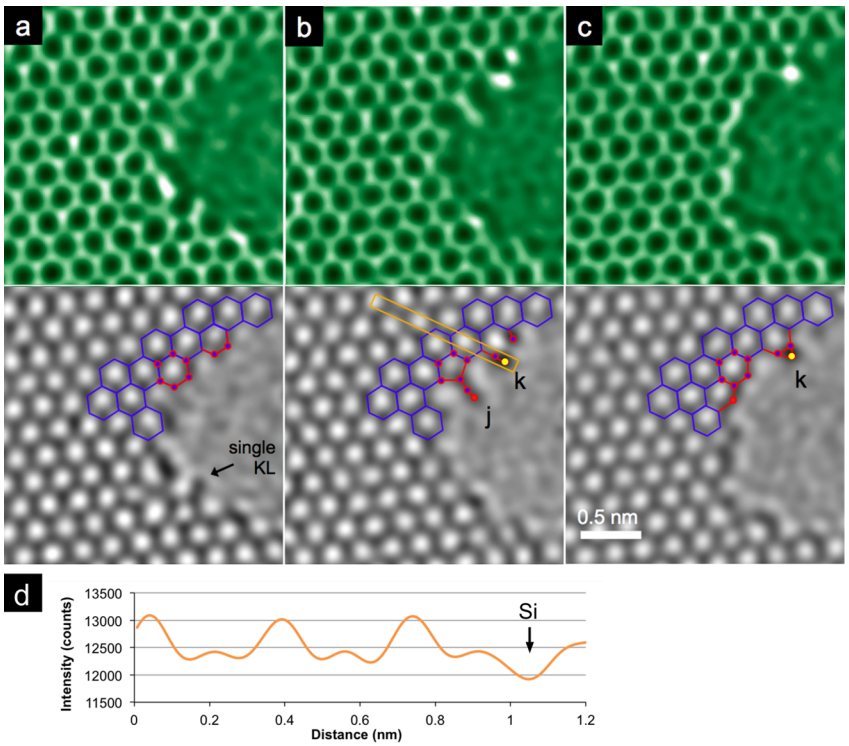

Figure 2. Series of AC-TEM images displayed without (top) and with (bottom) a schematic overlay of the dynamically evolving atomic structure. (a) Initial armchair edge formed from six-membered rings. (b) Two Klein edge doublets after 9 s of electron beam illumination. One KLD composed of an additional carbon atom schematically shown as a red spot (labeled *j*) and another KLD formed by an additional silicon atom shown as a yellow spot (labeled *k*). (c) Restitching of the KLDs into the graphene lattice after 8 s as one zigzag edge and one nonhexagonal mixed composition edge. (d) Box intensity profile of a 1.2 × 0.1 nm region around KLD labeled *k* as specified in (b), where atom positions are represented by dark intensity in the images, shown as depressions in the line profile. The arrow indicates the Si adatom position.

Following continuous e-beam irradiation for 8 s, the mixed composition KLD (labeled *k*) rebonds, recreating the hexagonal structure of the main lattice, but also forms a triangular bond between the Si and C atoms in a similar mechanism to that observed previously.[26] This illustrates another mechanism by which the local edge structure of the graphene is altered, as the local triangular edge configuration does not correspond to sp^2 hybridization. This mixed composition KLD formation and rebonding process is thus a candidate for use in graphene edge functionalization processes, as it occurs within a discrete regime of electron radiation exposure (2.3×10^7 e^-/nm^2 to 4.3×10^7 $e^- \cdot s/nm^2$), ending in a geometry less common for a graphene flake edge.

The KLDs also occur along zigzag-type graphene edges (Figure 3) with $x-y$ projection lengths of 0.24 and 0.21 ± 0.02 nm (or 1.7 and 1.5 times the length of a single C−C graphene bond), for the left and right side KLD, respectively. These KLDs appear to have been created in the zigzag edge environment by the displacement of an atom shared between two six-membered rings. However, after formation, the KLDs are sputtered from their original position near the main crystal.

The multislice simulation (Figure 3d) generated for imaging conditions matching the experiment at 80 kV ($C_3 = -10$ μm, $C_1 = 6$ nm)[49] shows a close match with the experimental data. However, there are subtle differences between experimental and simulated images, as the space between the two KLDs in the model used for the image simulations has a single dangling C atom remaining or a single KL present. This difference shows that the contrast of the single KL compared to the surrounding vacuum is unambiguous. However, in the experimental data the contrast of the C atom position between the KLDs is low enough to determine that a single KL is not present. In the case of the zigzag edge time series (Figure 3a−c), two C atoms, including one atom between the KLDs, have been locally ejected, greatly reducing the number of atoms present and making the self-healing process observed in the armchair edges impractical for zigzag edges. In contrast to armchair-environment KLDs, we propose that KLD formation on a zigzag edge is a pathway toward atom amputation, as verified by molecular dynamics simulations at high temperatures.[47]

The formation of a KLD in the self-healing armchair edge environment cannot be a coincidental arrangement arising from random single-atom knock-on events. The observation of KLDs is not a rare observation, and their existence over several seconds under continuous beam irradiation is exceptional compared to the picosecond time scale necessary to remove a KLD calculated in simulations.[47] It is therefore probable

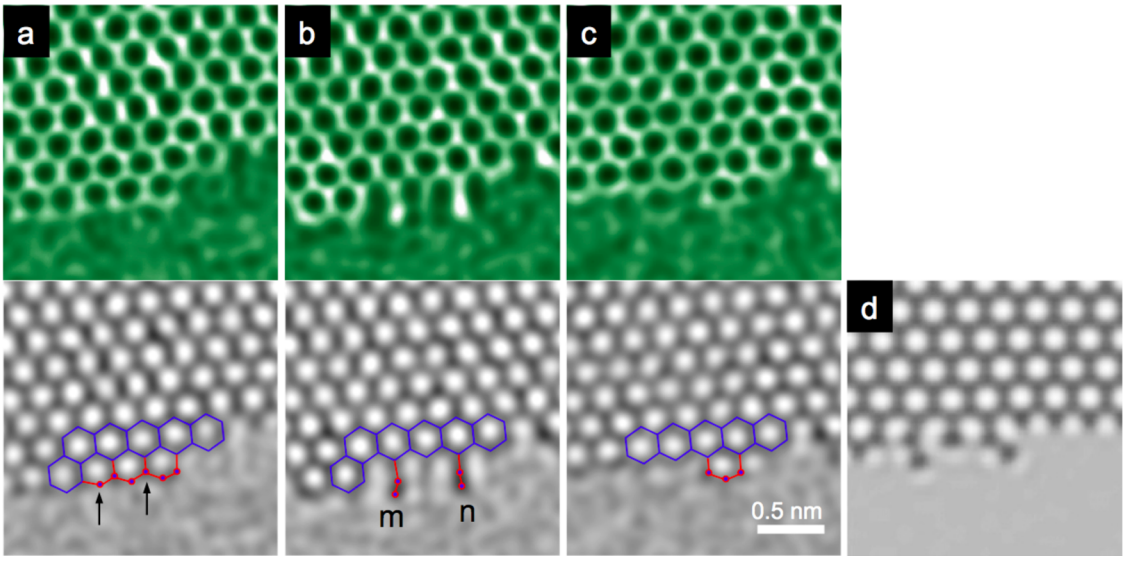

Figure 3. Time series of AC-TEM images revealing the formation of two Klein doublets along a zigzag edge showing (a) initial zigzag-type edge and (b) KLDs formed after 7 s of electron illumination. (c) After an additional 13 s the KLD-forming atoms have been sputtered. The bottom row of images includes schematic overlays of the processes occurring at the regions of interest. Arrows in (a) indicate C atoms that are locally sputtered prior to the formation of KLDs before the subsequent image (b) in the time series. (d) Simulated image[28] of the zigzag edge Klein doublets at C_1 = 6 nm.

that this is a semistable configuration and that the energy input from the 80 kV electron beam provides the activation energy required to switch between the armchair edge and KLD configurations.

The armchair environment KLD atoms along with all the variations of graphene edges eventually sputter away following extended irradiation with an 80 kV beam at 2.5 $\times$ 10^6 $e^- \cdot s/nm^2$. However, the presence of the KLD over several seconds may be one mechanism by which this new edge geometry contributes to the robustness and functionality of graphene edges.

CONCLUSIONS

The results presented here document the variation in local structure configurations surrounding Klein edge doublets and their influences on KLD stability. KLDs have been observed to exist for several seconds under continuous electron irradiation at both the armchair and zigzag monolayer graphene edge environments. The ability to restitch the KLD into the original hexagonal lattice at armchair edges along with supportive bond length studies[26] shows that the dangling KLD is not functionalized by hydrogen in these observations. The presence of a C–Si mixed-composition KLD that rebonds to the graphene lattice is a mechanism by which functionalization of the edge can be achieved. Finally, the KLD at the zigzag edge environment cannot be restitched to the graphene lattice because of the significant loss of neighboring carbon atoms, but shows that KLD formation is a mechanism that leads to atom abstraction.

METHODS

CVD graphene specimens supported by SiN grids were heated for approximately 24 h just prior to TEM observation at 180 °C and 1 $\times$ 10^{-3} Pa in order to remove residual hydrocarbons. Aberration-corrected TEM images were collected at room temperature using a double-aberration-corrected JEOL 2200MCO[38–40] operated at 80 kV acceleration voltage. Although equipped with a monochromator that can enhance images by removing chromatic effects, this work was done with the monochromator turned off for higher electron current density[37] micrographs. Images were collected with a negative spherical aberration coefficient $C_3 \approx -3$ μm to balance C_5[43] and with a defocus, C_1, between −3 and −6 nm. Images shown in Figures 1–3 are displayed with a low-pass fifth-order Butterworth filter to remove high-frequency information. The cut-off frequency was set to 110 $pixels^{-1}$ of the 2048 pixel images, equivalent to 0.288 nm in real space. The effect was to reduce the high spatial frequency information for easier characterization of the KLD position and orientation, but also causes some subtle features arising from Fourier-filtered noise in the vacuum region next to the specimen.

Conflict of Interest: The authors declare no competing financial interest.

Acknowledgment. Financial support from EPSRC (Platform Grants EP/F048009/1 and EP/K032518/1), The Royal Society, and JEOL Ltd. are gratefully acknowledged.

Supporting Information Available: The Supporting Information is available free of charge on the ACS Publications website at DOI: 10.1021/acsnano.5b02730.

Extended progression of time series data and discussion of contrast variations in the images (PDF)

REFERENCES AND NOTES

1. Novoselov, K. S.; Fal'ko, V. I.; Colombo, L.; Gellert, P. R.; Schwab, M. G.; Kim, K. A Roadmap for Graphene. *Nature* **2012**, *490*, 192–200.
2. Kobayashi, Y.; Fukui, K.; Enoki, T.; Kusakabe, K. Edge State on Hydrogen-Terminated Graphite Edges Investigated by

Scanning Tunneling Microscopy. *Phys. Rev. B: Condens. Matter Mater. Phys.* **2006**, *73*, 125415.
3. Suenaga, K.; Koshino, M. Atom-by-Atom Spectroscopy at Graphene Edge. *Nature* **2010**, *468*, 1088–1090.
4. Jia, X.; Hofmann, M.; Meunier, V.; Sumpter, B. G.; Campos-Delgado, J.; Romo-Herrera, J. M.; Son, H.; Hsieh, Y.-P.; Reina, A.; Kong, J.; et al. Controlled Formation of Sharp Zigzag and Armchair Edges in Graphitic Nanoribbons. *Science* **2009**, *323*, 1701–1705.
5. Cresti, A.; Roche, S. Edge-Disorder-Dependent Transport Length Scales in Graphene Nanoribbons: From Klein Defects to the Superlattice Limit. *Phys. Rev. B: Condens. Matter Mater. Phys.* **2009**, *79*, 233404.
6. Nakada, K.; Fujita, M.; Dresselhaus, G.; Dresselhaus, M. S. Edge State in Graphene Ribbons: Nanometer Size Effect and Edge Shape Dependence. *Phys. Rev. B: Condens. Matter Mater. Phys.* **1996**, *54*, 17954–17961.
7. Kobayashi, Y.; Fukui, K.; Enoki, T.; Kusakabe, K.; Kaburagi, Y. Observation of Zigzag and Armchair Edges of Graphite Using Scanning Tunneling Microscopy and Spectroscopy. *Phys. Rev. B: Condens. Matter Mater. Phys.* **2005**, *71*, 193406.
8. Ezawa, M. Peculiar Width Dependence of the Electronic Properties of Carbon Nanoribbons. *Phys. Rev. B: Condens. Matter Mater. Phys.* **2006**, *73*, 045432.
9. Son, Y.-W.; Cohen, M. L.; Louie, S. G. Energy Gaps in Graphene Nanoribbons. *Phys. Rev. Lett.* **2006**, *97*, 216803.
10. Wang, Z. F.; Li, Q.; Zheng, H.; Ren, H.; Su, H.; Shi, Q. W.; Chen, J. Tuning the Electronic Structure of Graphene Nanoribbons through Chemical Edge Modification: A Theoretical Study. *Phys. Rev. B: Condens. Matter Mater. Phys.* **2007**, *75*, 113406.
11. Han, M. Y.; Özyilmaz, B.; Zhang, Y.; Kim, P. Energy Band-Gap Engineering of Graphene Nanoribbons. *Phys. Rev. Lett.* **2007**, *98*, 206805.
12. Wassmann, T.; Seitsonen, A. P.; Saitta, A. M.; Lazzeri, M.; Mauri, F. Structure, Stability, Edge States, and Aromaticity of Graphene Ribbons. *Phys. Rev. Lett.* **2008**, *101*, 096402.
13. Ni, Z. H.; Chen, W.; Fan, X. F.; Kuo, J. L.; Yu, T.; Wee, A. T. S.; Shen, Z. X. Raman Spectroscopy of Epitaxial Graphene on a SiC Substrate. *Phys. Rev. B: Condens. Matter Mater. Phys.* **2008**, *77*, 115416.
14. Akola, J.; Heiskanen, H. P.; Manninen, M. Edge-Dependent Selection Rules in Magic Triangular Graphene Flakes. *Phys. Rev. B: Condens. Matter Mater. Phys.* **2008**, *77*, 193410.
15. Wang, X.; Ouyang, Y.; Li, X.; Wang, H.; Guo, J.; Dai, H. Room-Temperature All-Semiconducting Sub-10-Nm Graphene Nanoribbon Field-Effect Transistors. *Phys. Rev. Lett.* **2008**, *100*, 206803.
16. Kosynkin, D. V.; Higginbotham, A. L.; Sinitskii, A.; Lomeda, J. R.; Dimiev, A.; Price, B. K.; Tour, J. M. Longitudinal Unzipping of Carbon Nanotubes to Form Graphene Nanoribbons. *Nature* **2009**, *458*, 872–876.
17. Jiao, L.; Zhang, L.; Wang, X.; Diankov, G.; Dai, H. Narrow Graphene Nanoribbons from Carbon Nanotubes. *Nature* **2009**, *458*, 877–880.
18. Cai, J.; Ruffieux, P.; Jaafar, R.; Bieri, M.; Braun, T.; Blankenburg, S.; Muoth, M.; Seitsonen, A. P.; Saleh, M.; Feng, X.; et al. Atomically Precise Bottom-up Fabrication of Graphene Nanoribbons. *Nature* **2010**, *466*, 470–473.
19. Krivanek, O. L.; Chisholm, M. F.; Nicolosi, V.; Pennycook, T. J.; Corbin, G. J.; Dellby, N.; Murfitt, M. F.; Own, C. S.; Szilagyi, Z. S.; Oxley, M. P.; et al. Atom-by-Atom Structural and Chemical Analysis by Annular Dark-Field Electron Microscopy. *Nature* **2010**, *464*, 571–574.
20. Krauss, B.; Nemes-Incze, P.; Skakalova, V.; Biro, L. P.; von Klitzing, K.; Smet, J. H. Raman Scattering at Pure Graphene Zigzag Edges. *Nano Lett.* **2010**, *10*, 4544–4548.
21. Lü, X.; Zheng, Y.; Xin, H.; Jiang, L. Spin Polarized Electron Transport through a Graphene Nanojunction. *Appl. Phys. Lett.* **2010**, *96*, 132108.
22. Cocchi, C.; Ruini, A.; Prezzi, D.; Caldas, M. J.; Molinari, E. Designing All-Graphene Nanojunctions by Covalent Functionalization. *J. Phys. Chem. C* **2011**, *115*, 2969–2973.
23. Cocchi, C.; Prezzi, D.; Ruini, A.; Caldas, M. J.; Molinari, E. Optical Properties and Charge-Transfer Excitations in Edge-Functionalized All-Graphene Nanojunctions. *J. Phys. Chem. Lett.* **2011**, *2*, 1315–1319.
24. Hämäläinen, S. K.; Sun, Z.; Boneschanscher, M. P.; Uppstu, A.; Ijäs, M.; Harju, A.; Vanmaekelbergh, D.; Liljeroth, P. Quantum-Confined Electronic States in Atomically Well-Defined Graphene Nanostructures. *Phys. Rev. Lett.* **2011**, *107*, 236803.
25. Tao, C.; Jiao, L.; Yazyev, O. V.; Chen, Y.-C.; Feng, J.; Zhang, X.; Capaz, R. B.; Tour, J. M.; Zettl, A.; Louie, S. G.; et al. Spatially Resolving Edge States of Chiral Graphene Nanoribbons. *Nat. Phys.* **2011**, *7*, 616–620.
26. He, K.; Lee, G.-D.; Robertson, A. W.; Yoon, E.; Warner, J. H. Hydrogen-Free Graphene Edges. *Nat. Commun.* **2014**, *5*, 3040.
27. He, K.; Robertson, A. W.; Fan, Y.; Allen, C. S.; Lin, Y.-C.; Suenaga, K.; Kirkland, A. I.; Warner, J. H. Temperature Dependence of the Reconstruction of Zigzag Edges in Graphene. *ACS Nano* **2015**, *9*, 4786–4795.
28. Liu, Z.; Suenaga, K.; Harris, P. J. F.; Iijima, S. Open and Closed Edges of Graphene Layers. *Phys. Rev. Lett.* **2009**, *102*. DOI: 10.1103/PhysRevLett.102.015501
29. Girit, C. O.; Meyer, J. C.; Erni, R.; Rossell, M. D.; Kisielowski, C.; Yang, L.; Park, C.-H.; Crommie, M. F.; Cohen, M. L.; Louie, S. G.; et al. Graphene at the Edge: Stability and Dynamics. *Science* **2009**, *323*, 1705–1708.
30. Koskinen, P.; Malola, S.; Haekkinen, H. Evidence for Graphene Edges beyond Zigzag and Armchair. *Phys. Rev. B: Condens. Matter Mater. Phys.* **2009**, *80*. DOI: 10.1103/PhysRevB.80.073401
31. Kim, K.; Coh, S.; Kisielowski, C.; Crommie, M. F.; Louie, S. G.; Cohen, M. L.; Zettl, A. Atomically Perfect Torn Graphene Edges and Their Reversible Reconstruction. *Nat. Commun.* **2013**, *4*. DOI: 10.1038/ncomms3723
32. Ishigami, M.; Chen, J. H.; Cullen, W. G.; Fuhrer, M. S.; Williams, E. D. Atomic Structure of Graphene on SiO2. *Nano Lett.* **2007**, *7*, 1643–1648.
33. Ritter, K. A.; Lyding, J. W. The Influence of Edge Structure on the Electronic Properties of Graphene Quantum Dots and Nanoribbons. *Nat. Mater.* **2009**, *8*, 235–242.
34. Kvashnin, D. G.; Sorokin, P. B.; Brüning, J. W.; Chernozatonskii, L. A. The Impact of Edges and Dopants on the Work Function of Graphene Nanostructures: The Way to High Electronic Emission from Pure Carbon Medium. *Appl. Phys. Lett.* **2013**, *102*, 183112.
35. Son, Y.-W.; Cohen, M. L.; Louie, S. G. Half-Metallic Graphene Nanoribbons. *Nature* **2006**, *444*, 347–349.
36. Wu, Y. A.; Fan, Y.; Speller, S.; Creeth, G. L.; Sadowski, J. T.; He, K.; Robertson, A. W.; Allen, C. S.; Warner, J. H. Large Single Crystals of Graphene on Melted Copper Using Chemical Vapor Deposition. *ACS Nano* **2012**, *6*, 5010–5017.
37. Robertson, A. W.; Allen, C. S.; Wu, Y. A.; He, K.; Olivier, J.; Neethling, J.; Kirkland, A. I.; Warner, J. H. Spatial Control of Defect Creation in Graphene at the Nanoscale. *Nat. Commun.* **2012**, *3*, 1144.
38. Hutchison, J. L.; Titchmarsh, J. M.; Cockayne, D. J. H.; Doole, R. C.; Hetherington, C. J. D.; Kirkland, A. I.; Sawada, H. A Versatile Double Aberration-Corrected, Energy Filtered HREM/STEM for Materials Science. *Ultramicroscopy* **2005**, *103*, 7–15.
39. Nellist, P. D.; Kirkland, A. I. Applications of the Oxford-JEOL - Aberration-Corrected Electron Microscope. *Philos. Mag.* **2010**, *90*, 4751.
40. Mukai, M.; Kim, J. S.; Omoto, K.; Sawada, H.; Kimura, A.; Ikeda, A.; Zhou, J.; Kaneyama, T.; Young, N. P.; Warner, J. H.; et al. The Development of a 200 kV Monochromated Field Emission Electron Source. *Ultramicroscopy* **2014**, *140*, 37–43.
41. Egerton, R. f. Beam-Induced Motion of Adatoms in the Transmission Electron Microscope. *Microsc. Microanal.* **2013**, *19*, 479–486.
42. Meyer, J. C.; Eder, F.; Kurasch, S.; Skakalova, V.; Kotakoski, J.; Park, H. J.; Roth, S.; Chuvilin, A.; Eyhusen, S.; Benner, G.; et al. Accurate Measurement of Electron Beam Induced Displacement Cross Sections for Single-Layer Graphene. *Phys. Rev. Lett.* **2012**, *108*, 196102.

43. Chang, L. Y.; Chen, F. R.; Kirkland, A. I.; Kai, J. J. Calculations of Spherical Aberration-Corrected Imaging Behaviour. *J. Electron Microsc.* **2003**, *52*, 359–364.
44. Klein, D. J. Graphitic Polymer Strips with Edge States. *Chem. Phys. Lett.* **1994**, *217*, 261–265.
45. He, K.; Robertson, A. W.; Lee, S.; Yoon, E.; Lee, G.-D.; Warner, J. H. Extended Klein Edges in Graphene. *ACS Nano* **2014**, *8*, 12272–12279.
46. Kotakoski, J.; Santos-Cottin, D.; Krasheninnikov, A. V. Stability of Graphene Edges under Electron Beam: Equilibrium Energetics versus Dynamic Effects. *ACS Nano* **2012**, *6*, 671–676.
47. Lee, G.-D.; Wang, C. Z.; Yoon, E.; Hwang, N.-M.; Ho, K. M. Reconstruction and Evaporation at Graphene Nanoribbon Edges. *Phys. Rev. B: Condens. Matter Mater. Phys.* **2010**, *81*, 195419.
48. Robertson, A. W.; Montanari, B.; He, K.; Kim, J.; Allen, C. S.; Wu, Y. A.; Olivier, J.; Neethling, J.; Harrison, N.; Kirkland, A. I.; et al. Dynamics of Single Fe Atoms in Graphene Vacancies. *Nano Lett.* **2013**, *13*, 1468–1475.
49. Stadelmann, P. *JEMS, EMS Java Ver. 4*, http://cimewww.epfl.ch/people/stadelmann/jemswebsite/jems.html; 2014.